Carbohydrate Polymers 104 (2014) 223–230

Contents lists available at ScienceDirect

Carbohydrate Polymers

journal homepage: www.elsevier.com/locate/carbpol

Physico-chemical properties and thermal stability of microcrystalline cellulose isolated from Alfa fibres

Djalal Trache[a,*], André Donnot[b], Kamel Khimeche[a], Riad Benelmir[b], Nicolas Brosse[b]

[a] UER Chimie appliquée, Ecole Militaire Polytechnique, BP 17, Alger, Algeria
[b] LERMAB, Faculté des Sciences et Technologies, Université de Lorraine, Vandœuvre-lès-Nancy, France

ARTICLE INFO

Article history:
Received 13 November 2013
Received in revised form 10 January 2014
Accepted 16 January 2014
Available online 27 January 2014

Keywords:
Microcrystalline cellulose
Alfa fibres
Chemical treatment
Characterization
Thermal properties

ABSTRACT

In this study, microcrystalline cellulose (Alfa-MCC) was extracted from Alfa fibres using acid hydrolysis method. The molecular weight of the cellulose samples was determined by gel permeation chromatography. The crystallinities were studied by means of X-ray diffraction and solid state cross polarization magic angle spinning ^{13}C nuclear magnetic resonance spectroscopy, revealing that Alfa-MCC was more crystalline than the native cellulose isolated from Alfa fibres. The morphology of the celluloses was investigated using scanning electron microscopy, showing a compact structure and a rough surface. Furthermore, a good thermal stability was shown for Alfa-MCC. Based on these analyses, Alfa-MCC showed tremendous potential use as composites reinforcing agent, foods stabilizer and pharmaceutical additive.

1. Introduction

Alfa grass or esparto grass (*Stipa tenacissima* L.) is a perennial tussock grass widely distributed in semi-arid ecosystems of the southern and western Mediterranean basin, mainly in the Maghreb (García-Fayos & Gasque, 2006). The main components of these fibres are cellulose, hemicellulose and lignin. These fibres have traditionally been used as animal feed and raw material for paper industry (Ahrens et al., 1998; Bessadok, Marais, Gouanvé, Colasse, & Zimmerlin, 2007). Utilization of Alfa fibres to produce biodegradable composites and thermoplastic materials has been recently published (Ben Brahim & Ben Cheikh, 2007; Maafi, Malek, Tighzert, & Dony, 2010; Nadji, Diouf, Benaboura, Bedard, & Riedl, 2009; Paiva, Ammar, Campos, Cheikh, & Cunha, 2007).

The isolation and characterization of microcrystalline cellulose particles (MCC) have been described from various cellulosic sources (Abdullah, 1991; Adel, Abd El-Wahab, Ibrahim, & Al-Shemy, 2011; Bochek, Shevchuk, & Lavrent'ev, 2003; Ejikeme, 2008; Ilindra & Dhake, 2008; Jahan, Saeed, He, & Ni, 2011; Keshk & Mohamed, 2011; Mohamad Haafiz, Eichhorn, & Jawaid, 2013a) and using several processes of extraction including mechanical treatments (Hanna et al., 2001; Laka & Chernyavskaya, 2007; Liimatainen, Sirviö, Haapala, Hormi, & Niinimäki, 2011), biological treatments (Adel, Abd El-Wahab, Ibrahim, & Al-Shemy, 2010; Janardhnan & Sain, 2006), and chemical treatments, e.g., acid hydrolysis (see Adel et al., 2011; Ilindra & Dhake, 2008). All these methods lead to different types of MCC, depending on the cellulose raw materials, its pre-treatment, and more crucially on the disintegrating process itself. However, biological methods are desirable because glucose, a useful by-product, is generated; these methods are more expensive and lead to MCC products having a lower crystallinity. Thus, acid hydrolysis is the conventional method of choice for manufacturing MCC (Adel et al., 2011; Elanthikkal, Gopalakrishnapanicker, Varghese, & Guthrie, 2010; Hanna et al., 2001; Ilindra & Dhake, 2008).

Due to its excellent properties, MCC has generated much attention and interest during these few last decades in both academic and industrial fields. In nanocomposite materials, MCC as reinforcing agent is attracting an increasing interest because of its potential advantages such as renewability, biodegradability and high surface area for bonding with resins. In addition, MCC exhibits a broad capacity to allow tailoring or grafting of chemical species to improve the morphology, thermal and mechanical properties of resulting composites (Azizi Samir, Alloin, & Dufresne, 2005; Hoyos, Cristia, & Vazquez, 2013; Mathew, Oskman, & Sain, 2005; Petersson, Kvien, & Oksman, 2007, Mohamad Haafiz, Hassan, Zakaria, Inuwa, & Islam, 2013b; Sun, Lu, Liu, Zhang, & Zhang, 2014a). Because of its chemical inactivity, absence of toxicity, high sorption and great hygroscopicity, MCC has received great interest (1) in pharmaceutical formulations, as a potential direct compression excipient especially in the design and development of tablets of poorly compressible and soluble drug (Chamsai & Sriamornsak, 2013; Kalita, Nath, Ochubiojo, & Buragohain, 2013; Levis & Deasy, 2001; Mallick,

* Corresponding author. Tel.: +213 661808275; fax: +213 21863204.
E-mail address: djalaltrache@gmail.com (D. Trache).

0144-8617/$ – see front matter © 2014 Elsevier Ltd. All rights reserved.
http://dx.doi.org/10.1016/j.carbpol.2014.01.058

Pradhan, & Mahapatra, 2013; Oyeniyi & Itiola, 2012; Podczeck & Al-Muti, 2010), (2) in food industry, as stabilizer, emulsifier, thickener and gelling agents in several dairy compounds (Galal, Fatma, Ali, Jihan, & Sahar, 2010; Sanguansri & Augustin, 2006; Schuh, Allard, Herrmann, Gibis, & Kohlus, 2013). Therefore, additional information with regard to Alfa-MCC chemical structures and properties may certainly help the researchers to use Alfa fibres into beneficial above-mentioned applications.

To the best of our knowledge, the isolation and characterization of microcrystalline cellulose (Alfa-MCC) from Alfa fibres has never been described. In this work, MCC was extracted from Alfa fibres using acid hydrolysis method and was fully characterized through infrared spectroscopy (FTIR), scanning electron microscopy (SEM), X-ray diffraction (XRD), ^{13}C nuclear magnetic resonance spectroscopy (NMR), Gel permeation chromatography (GPC) and thermal analysis. The comparison of Alfa-MCC and commercial microcrystalline cellulose (C-MCC) was also established.

2. Materials and methods

2.1. Raw materials

Alfa fibres were collected from the Saïda area, in Algeria. As received, these fibres were preconditioned before cellulose extraction took place. The fibres were washed with distilled water several times and dried in an oven at 80 °C for 24 h. Then they were shopped in an approximate length of 5–10 mm and kept in a vacuum desiccator. Cellulose microcrystalline (Avicel®, MCC) was supplied by Merck. Hydrochloric acid (37%) and diethyl ether were purchased from VWR-Prolabo, sodium hypochlorite (NaClO) solution was provided from Alfa Aesar, ethanol and benzene were purchased from Sigma–Aldrich. All reagents are analysis grade and they were used without prior purification.

2.2. Characterization of the Alfa fibres

For the material under investigation, the moisture content was determined using a KERN MRS 120-3 Infra-red moisture analyser (drying at 105 °C to constant weight), the ash content was analyzed according to the standard method ASTM D-1102-84, hot water extracts were determined using the standard method ASTM D-1110-56, organic solvents extracts were analyzed using the standard method ASTM D-1107-56 modified by replacing benzene with toluene, the holocellulose content was determined according to ASTM D-1104-56, the lignin content was analyzed using ASTM D-1106-56 and, finally, the determination of α-cellulose was carried out according to ASTM D-1103-60. Consequently, Alfa fibres used are composed of 44.6% of pure cellulose, 67.3% of holocellulose, 21.5% of lignin, 3.9% of hot water extractives, 5.2% of organic solvents extractives, 2.2% of ash, and 4.8% of moisture content.

2.3. Pulping and bleaching

A cartridge containing 25 g of dried Alfa stems was placed in a Soxhlet equipped with 1000 mL round bottom flask. The sample was first subjected to extraction at 85 °C with 600 mL ethanol/toluene (2/1 (v/v)) mixture during 24 h (Nadji et al., 2009).

The pulping process was performed under atmospheric pressure. The dried Alfa stems were kept for 4 h at 85 °C in a 500 mL round bottom flask containing 300 mL of NaOH (1 mol/L), equipped with a reflux condenser and a magnetic stirrer. The obtained mixture was then immediately filtered. The residue was successively washed with 350 mL of NaClO solution (40 wt%) for 18 h at 30 °C, 250 mL of ethanol for 2 h at 30 °C and 250 mL of diethyl ether for 2 h at ordinary temperature (Maafi et al., 2010). After this treatment, the cellulose pulp was washed with distilled water until pH of 7 was reached. At last, the residue obtained was dried for 24 h at 60 °C.

2.4. Microcrystalline cellulose preparation

Dry cellulose was suspended in an aqueous acid, heated under reflux conditions and gentle stirring and then cooled down to room temperature in a further 30 min. The degraded cellulose was filtered off in a coarse sintered-glass-filter crucible and washed with acid-free distilled water. For removing the last traces of acid, an aqueous suspension of degraded cellulose was neutralized to pH 7 with aqueous NaOH (1 mol/L), filtered off again, washed with distilled water and dried for 24 h at 50 °C. The resultant Alfa-MCC was transformed into fine powder by using a grinder. The product obtained after drying was snowy-white in appearance.

The hydrolysis experiments were performed using the same method described in the literature (Chauchan, Sapkal, Sapkal, & Zamre, 2009; Hanna et al., 2001) using 2.5 mol/L of hydrochloric acid at 85 °C for 120 min with constant agitation in the ratio of 1:10 pulp over liquor.

2.5. Characterization

2.5.1. Fourier transform infrared spectroscopy analysis (FTIR)

The dried samples were embedded in KBr pellets and analyzed by using a Shimadzu spectrometer 8400S. The spectra were recorded in transmittance band mode in the range of 4000–600 cm^{-1}. 32 scans were co-added in order to achieve an acceptable signal-to-noise ratio. In all cases, spectra resolution was maintained at 4 cm^{-1}.

2.5.2. Cellulose samples purity determination

The chemical compositions of the three carbohydrate polymers were determined by hydrolysis method (El Hage, Chrusciel, Desharnais, & Brosse, 2010; Hamed, Fouad, Hamed, & Al-Hajj, 2012; Obama, Ricochon, Muniglia, & Brosse, 2012). Samples were hydrolysed with 72% (w/w) sulphuric acid for 1 h at 30 °C. After that, it was diluted to 3% (w/w) sulphuric acid by adding water and then autoclaved at 121 °C. Monosaccharide contents in the filtrate were quantified using anion-exchange chromatography with pulsed amperometric detector (HPAEC-PAD: Dionex ICS-3000 system). The dried residues obtained were weighted to give klason lignin content. The acid-soluble lignin content was determined from absorbance at 205 nm according to Lin and Dence (Lin & Dence, 1992).

2.5.3. Gel permeation chromatography (GPC) measurements

2.5.3.1. Samples preparation. The three cellulose samples were derivatized using phenyl isocyanate to obtain cellulose tricarbanilate (CTC). The tricarbanilation process was done using the procedure described by Foston (Foston, Hubbell, & Ragauskas, 2011) in the following way: 15 mg of the dried cellulose sample, placed in 25 mL flask, was treated with 4 mL anhydrous pyridine and 0.5 mL phenyl isocyanate, sealed with Teflon-lined cap. The reaction mixture was then kept in oil bath at 70 °C and allowed to stir for 48 h. After the reaction completed, the solution was cooled and 1 mL methanol was added to quench any remaining phenyl isocyanate. Subsequently, the mixture was poured into 100 mL methanol–water (7:3). The precipitated CTC was purified through centrifuging by repeated washing with methanol–water for 3 times, and water for 2 times. The CTC was then lyophilized.

Prior to each GPC analysis, Cellulose derivatives were dissolved in tetrahydrofuran (THF), filtered through a 0.45 μm teflon membrane and placed in a 2 mL auto-sampler vial.

To minimize a rough random error, four analyses of each sample were performed: two CTC solutions were prepared and each

solution was analyzed twice. The measurement error is thus the standard deviation calculated from four measurements.

2.5.3.2. Analyses. The number-average molecular weight (M_n) and weight-average molecular weight (M_w) were determined by GPC with a Dionex Ultimate-3000 HPLC system consisting of an autosampler and a UV detector and using THF as eluent. Standard polystyrene samples were used to construct a calibration curve. Data were collected and analyzed with Chromeleon software version 6.8 (Dionex Corp., USA). The analyses were carried out at 30 °C with a flow rate of 1 mL/min. The cellulose derivatives in the eluent were detected at the wavelength of 235 nm. The apparent number-average and weight-average DP_n and DP_w were calculated by dividing respectively M_n and M_w values by 519, the monomer equivalent weight of CTC.

2.5.4. Scanning electron microscopy (SEM)

SEM analyses were recorded by using Hitachi S-4800 scanning electron microscope. Samples were prepared by dispersing dry powder on double-sided conductive adhesive tape and they were coated with carbon by arc discharge method. Samples were scanned in secondary electrons (SE) for morphology.

2.5.5. X-ray diffraction analysis (XRD)

XRD analysis was carried out on different cellulose samples using a PANalytical X'Pert PRO Multi-Purpose Diffractometer with Cu Kα radiation. An X'Celerator detector was used to collect data over an angular range of 10–30°/2θ with a step size of 0.0170/2θ and a count time of 50.1650 s at each step. The voltage was chosen to be 45 kV with a current of 40 mA. Powdered specimens were prepared for X-ray diffraction analysis using the PANalytical powder sample preparation Kit and back-loaded into nickel-coated steel sample holders. The crystalline indexes of samples were calculated from X-ray diffraction patterns via Eq. (1) (Segal, Creely, Martin, & Conrad, 1959):

$$\mathrm{CrI} = \frac{I_{2\,00} - I_{\mathrm{am}}}{I_{200}} \quad (1)$$

where CrI is crystallinity index, I_{002} is the peak intensity of the 0 0 2 lattice plane (at about $2\theta = 22$) and I_{am} is the peak intensity of the amorphous phase which corresponds to the peak at about $2\theta = 18$.

The *d*-spacings were calculated using the Bragg's equation and the crystallite sizes were calculated from the Scherrer equation as follows:

$$L = \frac{k\lambda}{\beta \cos\theta} \quad (2)$$

where L is the size of crystallite (nm), k is the Scherrer constant (0.94), λ is the X-ray wavelength (0.15418 nm), β is the FWHM (full width half maximum) of the lattice plane reflection in radian, and θ is the corresponding Bragg angle (reflection angle) (He, Tang, & Wang, 2007).

2.5.6. ^{13}C NMR measurements

All solid state nuclear magnetic resonance employing the technique of cross-polarization magic angle spinning (CP/MAS) experiments were performed on a Bruker Avance-300 spectrometer (7.05 T), operating at a frequency of 76.46 MHz. The spectrometer was equipped with a 4-mm CP/MAS probe and the samples were pressed into cylindrical zirconia rotors and spun at magic angle at 7 kHz. The spectra were acquired using a spectra width of 30 kHz, a single pulse length of 6 μs, a recycled delay of 3 s, acquisition time of 0.04 s, contact time of 3 ms. The spectra were recorded as the sum of 4000 scans and calibrated using the methane carbon atoms of adamantane as an external standard ($\delta = 29.47$ ppm). ^{13}C data were processed offline using XWinNMR processing software with a line broadening of 10 Hz. The cellulose crystallinity index was calculated from the areas of the crystalline and amorphous C-4 signals using the following formula (Larsson, Westermark, Iversen, 1995). Typical errors for this analysis are 3% (standard deviation).

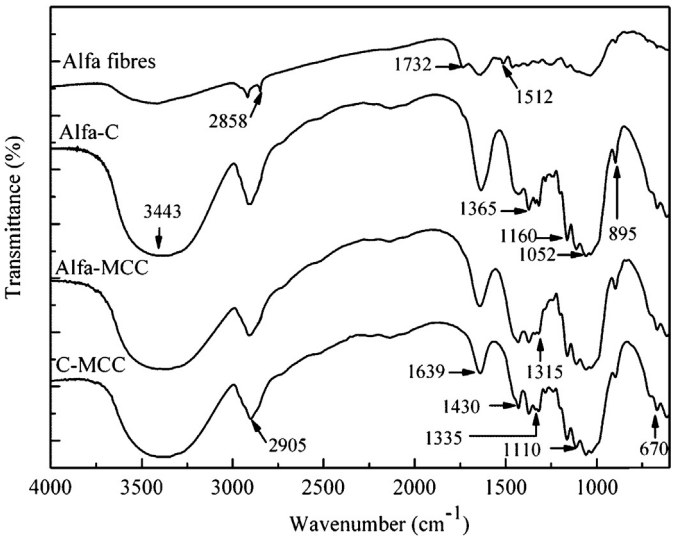

Fig. 1. FTIR spectra of Alfa fibres; Alfa-C, Alfa-MCC and C-MCC.

$$\mathrm{CrI} = \frac{A_{86-92\,\mathrm{ppm}}}{A_{79-86\,\mathrm{ppm}} + A_{86-92\,\mathrm{ppm}}} \quad (3)$$

2.5.7. Thermal stability analysis

There are only a few DSC studies in the literature (Leroy, Cancellieri, & Leoni, 2006; Lu & Hsieh, 2012; Mok & Antal, 1983; Moran, Alvarez, Cyras, & Vasquez, 2008; Sun, Sun, Zhao, & Sun, 2004; Sun, Sun, Fowler, & Baird, 2004; Yang, Yan, Chen, Lee, & Zheng, 2007) about the thermal decomposition of cellulose materials which is preferably studied by TGA. However, in this survey, a simultaneous DSC–TGA analyser model Setaram Setsys 12 was used. It is calibrated against melting points and fusion enthalpies of indium, tin, lead and zinc. The mass of each sample was in a range of 5–10 mg, which was heated from 50 to 700 °C under nitrogen gas atmosphere with two different heating rates (10, 15 K/min). Data acquisition and processing were done with Setsoft 2000 version 3.0 software.

3. Results and discussion

3.1. Chemical structure analysis with Infrared spectroscopy

FTIR spectra of Alfa fibres, Alfa-C, Alfa-MCC and commercial C-MCC samples are given in Fig. 1. In Alfa fibres spectrum, signal at 1732 cm^{-1} is assigned to the acetyl group of hemicellulose uronic ester or the carboxylic ester group of the ferulic ring and *p*-coumaric acid (Maafi et al., 2010). The peak at 1512 cm^{-1} is due to the presence of lignin (Nadji et al., 2009). A comparison between Alfa fibres and Alfa-C shows that the alkaline treatment disrupts the lignin structure and breaks the linkage between lignin and other carbohydrate fractions in Alfa fibres. The presence of a more crystalline order in microcrystalline cellulose samples (Alfa-MCC, C-MCC) can be confirmed by the shift of the spectra from 2901 cm^{-1} (C—H stretching vibration) to higher wavenumber value (2905 cm^{-1}) (Kalita et al., 2013). The band assigned to a symmetric CH_2 bending vibration, at 1430 cm^{-1} increased in microcrystalline cellulose samples. This band is also known as the crystallinity band

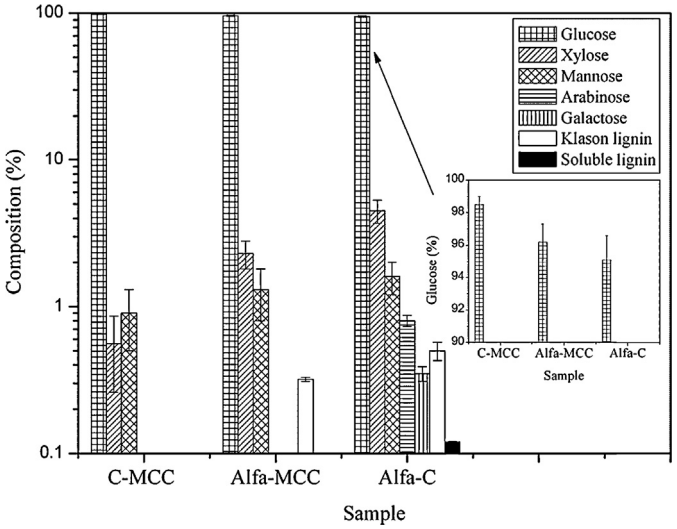

Fig. 2. Composition of the solid residues. All data are given as a percentage (w/w), with respect to initial dry weight of cellulose samples.

(Kalita et al., 2013), where an increase in its intensity demonstrates higher degree of crystallinity.

3.2. HPAEC-PAD analysis

HPAEC-PAD analyses of Alfa-C, Alfa-MCC and C-MCC were carried out to determine the cellulose purity and to quantitatively analyze their changes in composition, based on monomer content measured after an acid hydrolysis.

Fig. 2 gives the sugars concentrations in the liquid phases after hydrolysis. C-MCC and Alfa-MCC contain high cellulose contents (glucose >96%) and lower hemicelluloses contents than Alfa-C (glucose <95.5%). The values are in accordance with previous findings reported so far for microcrystalline cellulose (Leppänen, Andersson, Torkkeli, Knaapila, & Kotelnikova, 2009; Virtanen, Svedström, Andersson, Tervala, & Torkkeli, 2012). The lignin contents for Alfa-C and Alfa-MCC are very low (<1%), while no lignin is detected in C-MCC. These results show that the purity of Alfa-C, Alfa-MCC and C-MCC is higher than 95%.

3.3. Molecular weight distributions of cellulose samples

The M_w, M_n and polydispersity (M_w/M_n) of Alfa-C, Alfa-MCC and C-MCC were summarized in Table 1. So far, no data have been found in the literature regarding molecular weight distribution of Alfa grass-based celluloses. From Table 1, it is apparent that there was a reduction in molecular weight on Alfa-C fibres due to the depolymerisation of cellulose through the cleavage of glycosidic bonds.

These observations are in accordance with those reported in the literature for wood, cotton and bacterial celluloses (Eremeeva, 2003; Foston et al., 2011; Hubbell & Ragauskas, 2010; Shibazaki, Kuga, Onabe, & Brown, 1995). In addition, similar values of degree of polymerization and polydispersity for Alfa-MCC and C-MCC are observed; this indicated a relatively narrow molecular weight distribution.

3.4. Morphology of the cellulose samples

Fig. 3a, b and c show SEM micrographs of Alfa-C, Alfa-MCC and C-MCC, respectively. From Fig. 3a, after chemical treatment and bleaching (Alfa-C) it is clearly found that most of the plant's components are dissolved, leaving mainly the long, individualized, smooth

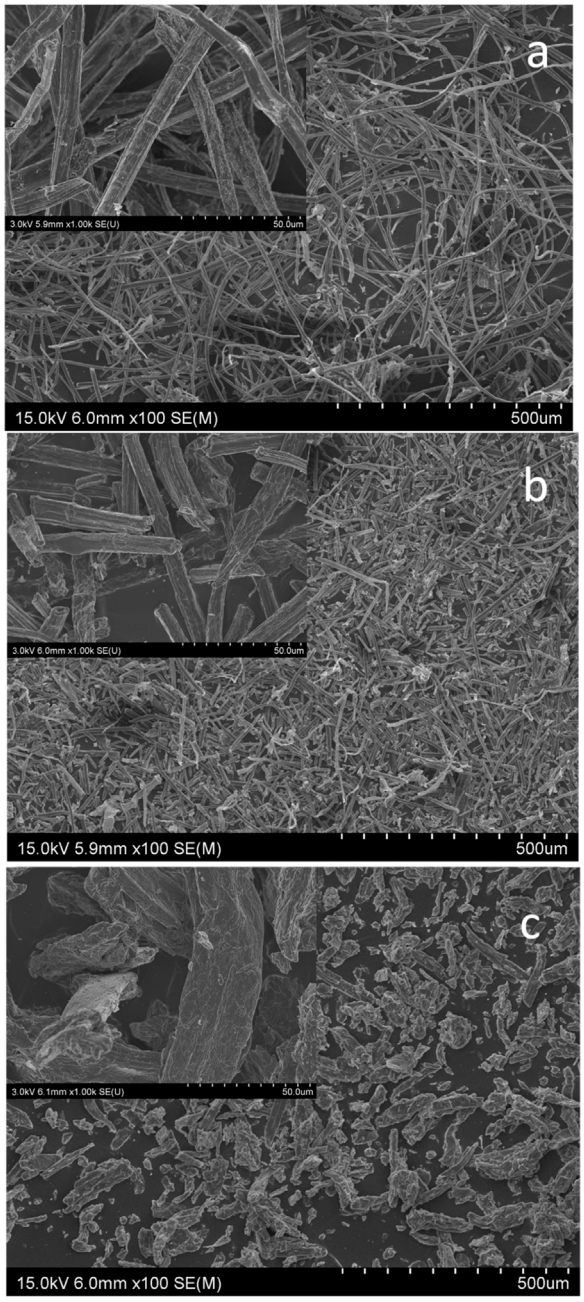

Fig. 3. SEM micrographs of (a) Alfa-C, (b) Alfa-MCC and (c) C-MCC samples.

fibres surface and uniform cellulose filaments. This observation is in accordance with the FTIR spectroscopic evidence of the removal of lignin and hemicellulose.

As shown from Fig. 3b, the Alfa-MCC particles exhibited short fibres strands with a rough surface morphology demonstrating that the fibres were altered after the chemical treatment. C-MCC (Fig. 3c) shows distinct crystalline shape of particles, smaller than Alfa-C.

The electron micrographs revealed that Alfa-C, Alfa-MCC cellulose filaments have diameters ranging from 5 to 10 μm while C-MCC filaments present higher diameters (from 10 to 20 μm). As reported earlier, this difference is probably due to the cellulose sources (Adel, Abd El-Wahab et al., 2011; Kalita et al., 2013; Paiva et al., 2007). Meanwhile, the fibre lengths of Alfa-MCC, C-MCC are in the same trend ranging from 20 to 200 μm.

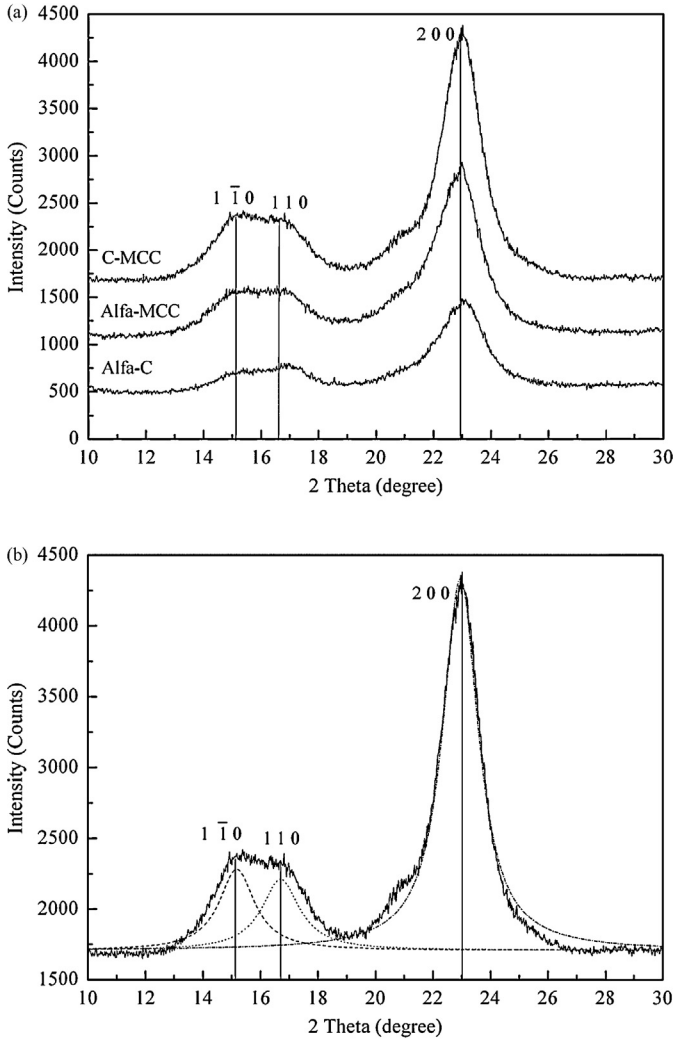

Fig. 4. (a) X-ray diffraction patterns of cellulose samples, (b) Peak separations of X-ray diffractometry profile of C-MCC.

3.5. Crystal structure analysis by X-ray diffraction and NMR

X-ray diffractograms for Alfa-C, Alfa-MCC and C-MCC are shown in Fig. 4a. Three main reflections at $2\theta = 15.2^{\circ}$, 16.8° and 22.6° were observed for all of the cellulose samples. Peak separations were carried out using Lorentzian deconvolution (Fig. 4b). The determination coefficients (r^2) were close to unity as given in Table 1.

The values for the *d*-spacing, the changes in the crystallinity and the crystallite sizes perpendicular to 1 $\bar{1}$ 0, 1 1 0 and 2 0 0 planes are summarized in Table 1. The increase in the crystallite sizes for the prepared Alfa-MCC particles in (1 $\bar{1}$ 0, 1 1 0 and 2 0 0), might be associated with a reduction in the corresponding amorphous region (Kim, Eom, & Wada, 2010; Poletto, Pistor, Zeni, & Zattera, 2011). Similar increase in crystal size on acid hydrolysis was reported by some researchers (Adel et al., 2010; Das, Ray, Bandyopadhyay, & Sengupta, 2010; Hanna et al., 2001).

CP/MAS ^{13}C NMR spectra and cellulose signal assignments are shown in Fig. 5a and b. Peaks have been assigned based on the literature and are displayed on the spectra (Foston et al., 2011; Larsson, Westermark, & Iversen, 1995). The peaks in the region between 60 and 105 ppm are due to the different carbons of cellulose. Signals from δ 86 to 92 ppm correspond to C-4 carbons from crystalline forms together with paracrystalline regions, whereas the broader up-field resonance from δ 80 to 86 ppm is assigned to amorphous regions. Crystallinity index of cellulose samples was determined using least-square line-fitting analysis of C-4 domain. According to literature methods (Foston et al., 2011; Larsson et al., 1995), Lorentzian lines were used for crystalline regions and Gaussian lines for the amorphous domains.

After acid hydrolysis of Alfa-C, the crystallinity index was increased of 23.7% and 24% using XRD and NMR analyses respectively (Table 1). The residual hemicellulose which is more amorphous than cellulose (consequently more accessible to the reactant) undergoes the breakdown (Lojewski, Zieba, Kolodziej, & Lojewska, 2011; Wan, Wang, & Xiao, 2010). The alkaline treatment used for cellulose extraction eliminates the major quantity of lignin and the acid hydrolysis process used for the preparation of microcrystalline cellulose removes the residual quantity of the amorphous lignin (Kumar, Hu, Hubbell, Ragauskas, & Wyman, 2013; Penkina, Hakola, Paaver, Vuorinen, & Kirsimäe, 2012). These results revealed that during acid hydrolysis, residual hemicelluloses in C-Alfa fibres were mostly dissolved and lignin-hemicellulose-cellulose interactions were also disrupted. Thus, acid hydrolysis was helpful to obtain high-purity cellulose without notable cellulose degradation.

Furthermore, it can be noticed from Table 1 that crystalline size and crystallinity index, obtained by the chemical treatment for Alfa-MCC are close to those obtained for the C-MCC.

3.6. Thermal stability analysis

Investigation on the thermal properties of cellulose fibres is important for future applications. Fig. 6a shows thermogravimetric analysis (TGA) and derivative thermograms (DTGA) curves for Alfa-C, Alfa-MCC and C-MCC samples. Table 2 reports the data obtained

Table 1
Parameters obtained from the GPC, XRD and NMR analyses for the cellulose samples studied.

Sample	M_n [a] (RSD%)	M_w [a] (RSD%)	DPI[a]	DP_n [a]	DP_w [a]	*d*-spacings (nm) [b]			*L* (nm) [c]			CrI (%) [d]	r^2
						1 $\bar{1}$ 0	1 1 0	2 0 0	1 $\bar{1}$ 0	1 1 0	2 0 0		
Alfa-C	78,215 (10)	438,004 (9)	5.59	150	844	0.573	0.537	0.389	3.992	3.954	3.949	59[e] 50[f]	0.9841[e] 0.9750[f]
Alfa-MCC	40,208 (8)	164,853 (6)	4.10	77	318	0.575	0.521	0.386	5.074	5.026	5.017	73[e] 62[f]	0.9864[e] 0.9915[f]
C-MCC	39,179 (7)	152,798 (8)	3.89	75	294	0.592	0.525	0.387	5.313	5.363	5.251	81[e] 69[f]	0.9879[e] 0.9882[f]

[a] M_n, number-average molecular weight; M_w, weight-average molecular weight; DPI, polydispersity index (M_w/M_n); DP_n, number-average degree of polymerization; DP_w, weight-average degree of polymerization; RSD, Relative Standard Deviation.
[b] *d*-spacings of typical three equatorial peaks of cellulose samples (using XRD analysis).
[c] Crystallite size perpendicular to each plane (using XRD analysis).
[d] Crystallinity index.
[e] Determined by XRD.
[f] Determined by NMR.

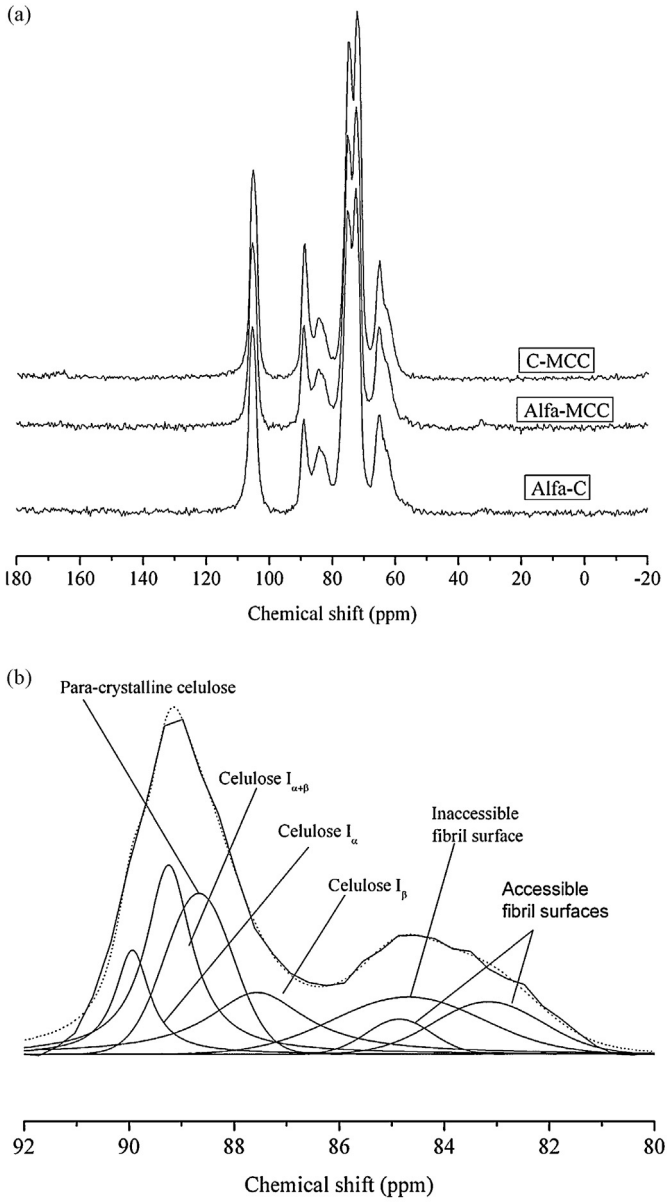

Fig. 5. (a) CP/MAS ^{13}C NMR spectrum of cellulose samples, (b) Spectral fitting for the C-4 region of CP/MAS ^{13}C NMR spectrum of C-MCC.

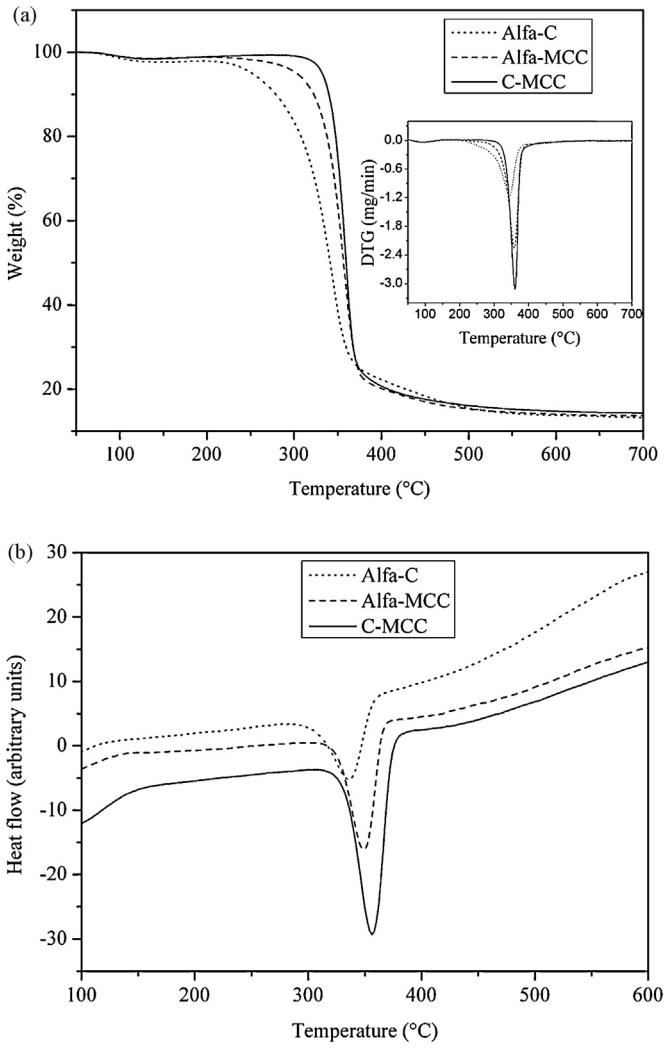

Fig. 6. (a) TGA/DTGA pyrolysis curves of cellulose samples, (b) DSC curves of cellulose samples; heating rate 15 °C/min.

from these curves. The TGA curves for all the samples show two stages of weight loss within the temperature range 20–700 °C. The drying stage for the samples occurs at a temperature range 60–140 °C approximately, which is due to the evaporation of water. For Alfa-C, within a wide range near 250–450 °C, a weight loss was observed due to degradation processes of cellulose, such as dehydration, decarboxylation, depolymerisation and decomposition of glycosyl units followed by the formation of a charred residue. For Alfa-MCC and C-MCC samples, an increase in decomposition temperatures compared to Alfa-C was observed. As previously described, this behaviour suggests that celluloses with higher crystallinity exhibit higher thermal stability (Kim et al., 2010; Poletto et al., 2011). Furthermore, it is interesting to point out that at 400 °C the weight loss for MCC samples is higher than Alfa-C, because of the lower purity of this latter (Elyounssi, Collar, Mateke, & Blin, 2012; Xiao, Sun, & Sun, 2001).

Further heating until 700 °C revealed that weight loss and residual weight of microcrystalline cellulose samples were higher than those of Alfa-C. This result is due to the higher amount of crystalline domains cellulose in MCC which are intrinsically flame resistant (Mandal & Chakrabarty, 2011).

The DSC curves shown in Fig. 6b, gave an endothermic peak, due to the volatilization of cellulose to levoglucosan and charring (Sullivan & Ball, 2012). From Tables 1 and 2, it is interesting to note that the heat of decomposition and the crystalline index have the same trend, which is attributed to the difficulty of the occurrence of heterolytic thermolysis of glycosidic bonds along the ordered chains (Sullivan & Ball, 2012). This decomposition process required high energy in the case of high degree of molecular ordering.

The decomposition of Alfa-C containing a small quantity of hemicelluloses presents a less pronounced shoulder or a large peak (Fig. 6a and b) instead of a well defined peak, because the temperature intervals for the hemicelluloses and cellulose decompositions partially overlaps each other. This shoulder is assigned to the volatilization of hemicelluloses and to a decrease of amorphous cellulose content (Popescu et al., 2010). For Alfa-MCC, it is clear that the decomposition peak is well resolved which confirms the elimination of hemicelluloses traces after hydrolysis. Moreover, no significant effect is caused by the lignin since its content is very low (<1%).

In view of the above results, it was concluded that the C-MCC and Alfa-MCC samples have good thermal stability and will be suitable

Table 2
Simultaneous TGA/DSC data obtained for the cellulose samples studied.

Sample	β (°C/min)	TGA analysis			DSC analysis		
		Onset (°C)[a]	Peak (°C)[b]	wt (%)[c]	T_i (°C)[d]	T_m (°C)[e]	ΔH (J/g)[f]
Alfa-C	10	288.43	332.71	73.25	284.95	328.59	270.51
	15	299.13	344.74	77.64	295.76	341.49	285.39
Alfa-MCC	10	322.15	351.39	80.16	318.78	348.86	327.83
	15	327.90	358.78	80.35	324.35	356.54	352.56
C-MCC	10	329.12	353.08	79.58	325.38	350.53	337.51
	15	335.67	360.61	79.88	331.48	358.78	357.45

[a] Onset decomposition temperature using TGA results.
[b] Peak temperature of DTGA.
[c] Residual weight at 400 °C.
[d] Onset decomposition temperature using DSC results.
[e] Peak temperature using DSC results.
[f] Heat of decomposition.

in the production of biocomposites, foods stabilizers and pharmaceutical compounds.

4. Conclusions

Microcrystalline cellulose prepared from Alfa fibres, one of the most abundant sources of cellulose in Algeria, has properties similar to those of commercial microcrystalline cellulose. FTIR and HPAEC-PAD analyses demonstrated that most hemicellulose and lignin of the raw fibres were removed during the extraction process. X-ray diffraction and NMR of the various cellulose samples revealed that acid hydrolysis of Alfa-C significantly increased overall crystallinity, due to preferential degradation of the amorphous components. The microcrystalline cellulose sample prepared exhibits improved thermal stability properties, thus making it promising candidate for use in many fields. It can be concluded from these results that the microcrystalline cellulose sample obtained from Alfa fibres has great potential applications in reinforced-polymer composites, pharmaceuticals and food industry.

References

Abdullah, A. B. M. (1991). Production of jute microcrystalline cellulose. *Journal of Bangladesh Academy of Science*, *15*(2), 85–87.

Adel, A. M., Abd El-Wahab, H. Z., Ibrahim, A. A., & Al-Shemy, M. T. (2010). Characterization of microcrystalline cellulose prepared from lignocellulosic materials. Part I. Acid catalyzed hydrolysis. *Bioresource Technology*, *101*, 4446–4455.

Adel, A. M., Abd El-Wahab, H. Z., Ibrahim, A. A., & Al-Shemy, M. T. (2011). Characterization of microcrystalline cellulose prepared from lignocellulosic materials. Part II: Physicochemical properties. *Carbohydrate Polymers*, *83*, 676–687.

Ahrens, F. W., Gulya, T., Worry, G. L., & Wright, W. P. (1998). *Papermaking fabric, process for producing high bulk products and the products produced thereby*. US Patent 5, 853,547.

Azizi Samir, M. A. S., Alloin, F., & Dufresne, A. (2005). Review of recent research into cellulosic whiskers, their properties and their application in nanocomposite field. *Biomacromolecules*, *6*(2), 612–626.

Ben Brahim, S., & Ben Cheikh, R. (2007). Influence of fibre orientation and volume fraction on the tensile properties of unidirectional Alfa-polyester composite. *Composites Science and Technology*, *67*, 140–147.

Bessadok, A., Marais, S., Gouanvé, F., Colasse, L., Zimmerlin, I., et al. (2007). Effect of chemical treatments of Alfa (*Stipa tenacissima*) fibres on water-sorption properties. *Composites Science and Technology*, *67*, 685–697.

Bochek, A. M., Shevchuk, I. L., & Lavrent'ev, V. N. (2003). Fabrication of microcrystalline and powdered cellulose from short flax fiber and flax straw. *Russian Journal of Applied Chemistry*, *76*(10), 1679–1682.

Chamsai, B., & Sriamornsak, P. (2013). Novel disintegrating microcrystalline cellulose pellets with improved drug dissolution performance. *Powder Technology*, *233*, 278–285.

Chauchan, P. Y., Sapkal, R. S., Sapkal, V. S., & Zamre, G. S. (2009). Microcrystalline cellulose from cotton rags (waste from garment and hosiery industries). *International Journal of Chemical Sciences*, *7*(2), 681–688.

Das, K., Ray, D., Bandyopadhyay, N. R., & Sengupta, S. (2010). Study of the properties of microcrystalline cellulose particles from different renewable resources by XRD, FTIR, nanoindentation, TGA and SEM. *Journal of Polymer Environment*, *18*, 355–363.

Ejikeme, P. M. (2008). Investigation of the physicochemical properties of microcrystalline cellulose from agricultural wastes I: Orange mesocarp. *Cellulose*, *15*, 141–147.

Elanthikkal, S., Gopalakrishnapanicker, U., Varghese, S., & Guthrie, J. T. (2010). Cellulose microfibres produced from banana plant wastes: Isolation and characterization. *Carbohydrate Polymers*, *80*, 852–859.

El Hage, R., Chrusciel, L., Desharnais, L., & Brosse, N. (2010). Effect of autohydrolysis of Miscanthus x giganteus on lignin structure and organosolv delignification. *Bioresource Technology*, *101*, 9321–9329.

Elyounssi, K., Collar, F. X., Mateke, J. N., & Blin, J. (2012). Improvement of charcoal yield by two-step pyrolysis on eucalyptus wood: A thermogravimetric study. *Fuel*, *96*, 161–167.

Eremeeva, T. (2003). Size-exclusion chromatography of enzymatically treated cellulose and related polysaccharides: A review. *Journal of Biochemical and Biophysical Methods*, *56*, 253–264.

Foston, M. B., Hubbell, C. A., & Ragauskas, A. J. (2011). Cellulose isolation methodology for NMR analysis of cellulose ultrastructure. *Materials*, *4*, 1985–2002.

Galal, A. M. N., Fatma, A. M. H., Ali, K. E., Jihan, M. K., & Sahar, H. S. M. (2010). Utilization of microcrystalline cellulose prepared from rice straw in manufacture of yoghurt. *Journal of American Science*, *6*(10), 226–231.

García-Fayos, P., & Gasque, M. (2006). Seed vs. microsite limitation for seedling emergence in the perennial grass *Stipa tenacissima* L. (Poaceae). *Acta Oecologica*, *30*, 276–282.

Hamed, O. A., Fouad, Y., Hamed, E. M., & Al-Hajj, N. (2012). Cellulose powder from olive industry solid waste. *BioResources*, *7*(3), 4190–4201.

Hanna, M., Biby, G., & Miladinove, V. (2001). *Production of microcrystalline cellulose by reactive extrusion*. US Patent 6,228,213.

He, J., Tang, Y., & Wang, S. Y. (2007). Differences in morphological characteristics of bamboo fibres and other natural cellulose fibres: studies on X-ray diffraction, solid state 13C-CP/MAS NMR, and second derivative FTIR spectroscopy data. *Iranian Polymer Journal*, *16*(12), 807–818.

Hoyos, C. G., Cristia, E., & Vazquez, A. (2013). Effect of cellulose microcrystalline particles on properties of cement based composites. *Materials and Design*, *51*, 810–818.

Hubbell, C., & Ragauskas, A. J. (2010). Effect of acid-chlorite delignification on cellulose degree of polymerization. *Bioresource Technology*, *101*(19), 7410–7415.

Ilindra, A., & Dhake, J. D. (2008). Microcrystalline cellulose from bagasse and rice straw. *Indian Journal of Chemical Technology*, *15*, 497–499.

Jahan, M. S., Saeed, A., He, Z., & Ni, Y. (2011). Jute as raw materials for the preparation of microcrystalline cellulose. *Cellulose*, *18*, 451–459.

Janardhnan, S., & Sain, M. M. (2006). Isolation of cellulose microfibrils – An enzymatic approach. *BioResources*, *1*(2), 176–188.

Kalita, R. D., Nath, Y., Ochubiojo, M. E., & Buragohain, A. K. (2013). Extraction and characterization of microcrystalline cellulose from fodder grass; *Setaria glauca* (L) P. Beauv, and its potential as a drug delivery vehicle for isoniazid, a first line antituberculosis drug. *Colloids and Surfaces B: Biointerfaces*, *108*, 85–89.

Keshk, S. M. A. S., & Mohamed, A. H. (2011). A new method for producing microcrystalline cellulose from *Gluconacetobacter xylinus* ans kenaf. *Carbohydrate Polymer*, *84*, 1301–1305.

Kim, U. J., Eom, S. H., & Wada, M. (2010). Thermal decomposition of native cellulose: Influence on crystallite size. *Polymer Degradation and Stability*, *95*, 778–781.

Kumar, R., Hu, F., Hubbell, C. A., Ragauskas, A., & Wyman, J. C. E. (2013). Comparison of laboratory delignification methods, their selectivity, and impacts on physiochemical characteristics of cellulosic biomass. *Bioresource Technology*, *130*, 372–381.

Larsson, P. T., Westermark, U., & Iversen, T. (1995). Determination of the cellulose I_α allomorph content in a tunicate cellulose by CP/MAS ^{13}C-NMR spectroscopy. *Carbohydrate Research*, *278*, 339–343.

Leppänen, K., Andersson, S., Torkkeli, M., Knaapila, M., Kotelnikova, N., et al. (2009). Structure of cellulose and microcrystalline cellulose from various wood species, cotton and flax studied by X-ray scattering. *Cellulose*, *16*, 999–1015.

Leroy, V., Cancellieri, D., & Leoni, E. (2006). Thermal degradation of lingo-cellulosic fuels: DSC and TGA studies. *Thermochimica Acta*, *451*, 131–138.

Levis, S. R., & Deasy, P. B. (2001). Pharmaceutical applications of size reduced grades of surfactant co-processed microcrystalline cellulose. *International Journal of Pharmaceutics*, *230*(1–2), 25–33.
Liimatainen, H., Sirviö, J., Haapala, A., Hormi, O., & Niinimäki, J. (2011). Characterization of highly accessible cellulose microfibers generated by wet stirred media milling. *Carbohydrate Polymers*, *83*, 2005–2010.
Lin, S. Y., & Dence, C. X. (1992). *Methods in lignin chemistry*. Berlin Heidelberg: Springer Series in Wood Science, Springer Verlag.
Lojewski, T., Zieba, K., Kolodziej, A., & Lojewska, J. (2011). Following cellulose depolymerization in paper: comparison of size exclusion chromatography techniques. *Cellulose*, *18*, 1349–1363.
Lu, P., & Hsieh, Y. L. (2012). Cellulose isolation and core-shell nanostructures of cellulose nanocrystals from chardonnay grape skins. *Carbohydrate Polymers*, *87*, 2546–2553.
Maafi, E. M., Malek, F., Tighzert, L., & Dony, P. (2010). Synthesis of polyurethane and characterization of its composites based on alfa cellulose fibers. *Journal of Polymer Environment*, *18*, 638–646.
Mallick, S., Pradhan, S., & Mahapatra, R. (2013). Effect of microcrystalline cellulose based comilled powder on compression and dissolution of ibuprofen. *International Journal of Biological Macromolecules*, *60*, 148–155.
Mandal, A., & Chakrabarty, D. (2011). Isolation of nanocellulose from waste sugarcane bagasse (SCB) and its characterization. *Carbohydrate Polymers*, *86*, 1291–1299.
Mathew, A. P., Oskman, K., & Sain, M. (2005). Mechanical properties of biodegradable composites from poly lactic acid (PLA) and microcrystalline cellulose (MCC). *Journal of Applied Polymer Science*, *97*, 2025–3014.
Mohamad Haafiz, M. K., Eichhorn, S. J., & Jawaid, M. (2013). Isolation and characterization of microcrystalline cellulose from oil palm biomass residue. *Carbohydrate Polymers*, *93*, 628–634.
Mohamad Haafiz, M. K., Hassan, A., Zakaria, Z., Inuwa, I. M., Islam, M. S., et al. (2013). Properties of polylactic acid composites reinforced with oil palm biomass microcrystalline cellulose. *Carbohydrate Polymers*, *98*, 139–145.
Mok, W. S. L., & Antal, M. J., Jr. (1983). Effects of pressure on biomass pyrolysis. II. Heats of reaction of cellulose pyrolysis. *Thermochimica Acta*, *68*, 165–186.
Moran, J., Alvarez, V., Cyras, V., & Vasquez, A. (2008). Extraction of cellulose and preparation of nanocellulose from sisal fibers. *Cellulose*, *15*(1), 149–159.
Nadji, H., Diouf, P. N., Benaboura, A., Bedard, Y., Riedl, B., et al. (2009). Comparative study of lignins isolated from Alfa grass (*Stipa tenacissima* L.). *Bioresource Technology*, *100*, 3585–3592.
Obama, P., Ricochon, G., Muniglia, L., & Brosse, N. (2012). Combination of enzymatic hydrolysis and organosolv pretreatments: Effect on lignin structures, delignification yields and cellulose- to-glucose conversion. *Bioresource Technology*, *112*, 156–163.
Oyeniyi, Y. J., & Itiola, O. A. (2012). The physicochemical characteristic of microcrystalline cellulose, derived from sawdust, agricultural waste products. *International Journal of Pharmacy and Pharmaceutical Sciences*, *4*, 197–200.
Paiva, M. C., Ammar, I., Campos, A. R., Cheikh, R. B., & Cunha, A. M. (2007). Alfa fibres: Mechanical, morphological and interfacial characterization. *Composites Science and Technology*, *67*, 1132–1138.
Petersson, L., Kvien, I., & Oksman, K. (2007). Structure and thermal properties of polylactic acid/cellulose wiskers nanocomposites materials. *Composites Science and Technology*, *67*, 2535–2544.
Penkina, A., Hakola, M., Paaver, U., Vuorinen, S., Kirsimäe, K., et al. (2012). Solid-state properties of softwood lignin and cellulose isolated by a new acid precipitation method. *International Journal of Biological Macromolecules*, *51*, 939–945.
Podczeck, F., & Al-Muti, E. (2010). The tensile strength of bilayered tablets made from different grades of microcrystalline cellulose. *European Journal of Pharmaceutical Sciences*, *41*, 483–488.
Poletto, M., Pistor, V., Zeni, M., & Zattera, A. J. (2011). Crystalline properties and decomposition kinetics of cellulose fibers in wood pulp obtained by two pulping processes. *Polymer Degradation and Stability*, *96*, 679–685.
Sanguansri, P., & Augustin, M. A. (2006). Nanoscale materials development – A food industry perspective. *Trends in Food Science & Technology*, *17*(10), 547–556.
Schuh, V., Allard, K., Herrmann, K., Gibis, M., Kohlus, R., et al. (2013). Impact of carboxymethyl cellulose (CMC) and microcrystalline cellulose (MCC) on functional characteristics of emulsified sausages. *Meat Science*, *93*, 240–247.
Segal, L., Creely, J. J., Martin, A. E., & Conrad, C. M. (1959). An empirical method for estimating the degree of crystallinity of native cellulose using the X-ray diffractometer. *Textile Research Journal*, *29*(10), 786–794.
Shibazaki, H., Kuga, S., Onabe, F., & Brown, R. M., Jr. (1995). Acid hydrolysis behaviour of microbial cellulose II. *Polymer*, *36*(26), 4971–4976.
Sullivan, A. L., & Ball, R. (2012). Thermal decomposition and combustion chemistry of cellulosic biomass. *Atmospheric Environment*, *47*, 133–141.
Sun, X., Lu, C., Liu, Y., Zhang, W., & Zhang, X. (2014). Melt-processed poly (vinyl alcohol) composites filled with microcrystalline cellulose from waste cotton fabrics. *Carbohydrate Polymers*, *101*, 642–649.
Sun, J. X., Sun, X. F., Zhao, H., & Sun, R. C. (2004). Isolation and characterization of cellulose from sugarcane bagasse. *Polymer Degradation and Stability*, *84*, 331–339.
Sun, X. F., Sun, R. C., Fowler, P., & Baird, M. S. (2004). Isolation and characterization of cellulose obtained by two-stage treatment with organosolv and cyanamide activated hydrogen peroxide from wheat straw. *Carbohydrate Polymers*, *55*, 379–391.
Virtanen, T., Svedström, K., Andersson, S., Tervala, L., Torkkeli, M., et al. (2012). A physico-chemical characterisation of new raw materials for microcrystalline cellulose manufacturing. *Cellulose*, *19*, 219–235.
Wan, J., Wang, Y., & Xiao, Q. (2010). Effects of hemicellulose removal on cellulose fiber structure and recycling characteristics of eucalyptus pulp. *Bioresource Technology*, *101*, 4577–4583.
Xiao, B., Sun, X. F., & Sun, R. C. (2001). Chemical, structural, and thermal characterizations of alkali-soluble lignins and hemicelluloses, and cellulose from maize stems, rye straw, and rice straw. *Polymer Degradation and Stability*, *74*, 307–319.
Yang, H., Yan, R., Chen, H., Lee, D. H., & Zheng, C. (2007). Characteristics of hemicellulose, cellulose and lignin pyrolysis. *Fuel*, *86*, 1781–1788.